5358 *Chem. Mater.* **2010,** *22,* 5358–5365
DOI:10.1021/cm1016799

CHEMISTRY OF MATERIALS
Article

Quantitative Design of Glassy Materials Using Temperature-Dependent Constraint Theory

Morten M. Smedskjaer,[†] John C. Mauro,*[,‡] Sabyasachi Sen,[§] and Yuanzheng Yue*[,†]

[†]*Section of Chemistry, Aalborg University, DK-9000 Aalborg, Denmark,* [‡]*Science and Technology Division, Corning Incorporated, Corning, New York 14831, and* [§]*Department of Chemical Engineering and Materials Science, University of California−Davis, Davis, California 95616*

Received June 16, 2010. Revised Manuscript Received August 11, 2010

The computational design of new materials has long been a "holy grail" within the materials chemistry community. However, accurate prediction of glass properties from first principles is often impossible, because of computational restrictions. Here, we present an alternative analytical modeling approach that focuses on the topology of the glass network. Specifically, we demonstrate the use of a temperature-dependent constraint model to enable accurate prediction of dynamic properties, taking the ternary soda−lime−borate glassy system as an example. Borate glasses have posed a particular challenge for traditional molecular dynamics simulations, because of the change in boron coordination that occurs in the presence of network modifiers. Focusing on topological constraints instead of interatomic force fields, the calculated compositional trends with our model are in quantitative agreement with experimental measurements. Our modeling approach enables the exploration of new composition spaces of glassy materials and is proving to be a valuable tool for revealing the topological source of properties such as liquid fragility, which has been a longstanding problem in condensed matter science.

1. Introduction

For many years, scientists have sought predictive methods for tailoring the properties of materials.[1−4] Despite considerable progress in computational materials chemistry, there has been no major breakthrough in the quantitative design of glassy materials, because of the complicated noncrystalline structure of glass and the long time scales involved with glass transition and relaxation phenomena. Such modeling is further complicated by the wide range of structural and dynamic heterogeneities in glass.[5−9] Recently, Kerner and Phillips[3,4] demonstrated that analytical modeling based on simple topological counting arguments can be used to predict the optimum glass-forming composition within the soda−lime−silicate system without using any adjustable fitting parameters. In this work, we present a comprehensive study applying temperature-dependent constraint theory to predict dynamic properties such as glass transition temperature (T_g) and fragility (m), thereby providing a powerful analytical tool for designing new glassy materials. We choose the soda−lime−borate ternary ($Na_2O-CaO-B_2O_3$) as the object of this study, since borate glasses contain an abundance of interesting structural and topological features (e.g., boron speciation[10−17] and heterogeneous distribution of network modifiers).[18] The theory is further developed in a manner to consider structural heterogeneities during the prediction of dynamic glassy properties.

Following the original work of Phillips and Thorpe,[19−21] the atomic structure of a glass may be treated as a network of bond constraints. According to this view, the network can be floppy (underconstrained), isostatic (optimally constrained), or stressed rigid (overconstrained), depending on the relative difference between the network dimensionality (d) and the average number (n) of constraints per atom.[19−21] When $n < d$, the network is underconstrained and contains low-frequency deformation modes (so-called

*Authors to whom correspondence should be addressed. E-mail: mauroj@corning.com (J.C.M.), yy@bio.aau.dk (Y.Y.).

(1) Martin, J. D.; Goettler, S. J.; Fosse, N.; Iton, L. *Nature* **2002**, *419*, 381–384.
(2) Salmon, P. S. *Nat. Mater.* **2002**, *1*, 87–88.
(3) Kerner, R.; Phillips, J. C. *Solid State Commun.* **2000**, *117*, 47–51.
(4) Kerner, R. *Models of Agglomeration and Glass Transition*; Imperial College Press: London, U.K., 2007.
(5) Tanaka, H.; Kawasaki, T.; Shintani, H.; Watanabe, K. *Nat. Mater.* **2010**, *9*, 324–331.
(6) Du, L. S.; Stebbins, J. F. *Chem. Mater.* **2003**, *15*, 3913–3921.
(7) Gaskell, P. H.; Eckersley, M. C.; Barnes, A. C.; Chieux, P. *Nature* **1991**, *350*, 675–677.
(8) Farnan, I.; Grandinetti, P. J.; Baltisberger, J. H.; Stebbins, J. F.; Werner, U.; Eastman, M. A.; Pines, A. *Nature* **1992**, *358*, 31–35.
(9) Elliott, S. R. *Nature* **1991**, *354*, 445–452.
(10) Silver, A. H.; Bray, P. J. *J. Chem. Phys.* **1958**, *29*, 984–990.
(11) Bray, P. J.; O'Keefe, J. G. *Phys. Chem. Glasses* **1963**, *4*, 37–46.
(12) Jellison, G. E.; Feller, S. A.; Bray, P. J. *Phys. Chem. Glasses* **1978**, *19*, 52–53.
(13) Bray, P. J. *J. Non-Cryst. Solids* **1987**, *95−96*, 45–59.
(14) Mozzi, R. L.; Warren, B. E. *J. Appl. Crystallogr.* **1970**, *3*, 251–257.
(15) Chason, E.; Spaepen, F. *J. Appl. Phys.* **1988**, *64*, 4435–4449.
(16) Yiannopoulos, Y. D.; Chryssikos, G. D.; Kamitsos, E. I. *Phys. Chem. Glasses* **2001**, *42*, 164–172.
(17) Walrafen, G. E.; Samanta, S. R.; Krishnan, P. N. *J. Phys. Chem.* **1980**, *72*, 113–120.
(18) Greaves, G. N.; Sen, S. *Adv. Phys.* **2007**, *56*, 1–166.
(19) Phillips, J. C. *J. Non-Cryst. Solids* **1979**, *34*, 153–181.
(20) Phillips, J. C.; Thorpe, M. F. *Solid State Commun.* **1985**, *53*, 699–702.
(21) He, H.; Thorpe, M. F. *Phys. Rev. Lett.* **1985**, *54*, 2107–2110.

 Published on Web 08/31/2010

"floppy modes"). The network is optimally rigid when $n = d$ and stressed rigid when $n > d$. Since the pioneering work of Phillips and Thorpe, constraint theory has been extensively studied.[22−28] Recently, Gupta and Mauro[29,30] developed a novel approach to the topological modeling of glass-forming liquids that accounts for the temperature-dependent nature of the network constraints. They successfully applied this temperature-dependent constraint approach to predict the scaling of the glass transition temperature (T_g) and fragility (m) with composition (x) in binary germanium selenide[29] and alkali borate[30] systems. ^{77}Se NMR spectroscopy studies on germanium selenide liquids have recently provided experimental evidence for the temperature dependence of network constraints.[31]

The Gupta−Mauro approach[29,30] formulates shear viscosity ($\eta(T,x)$) in terms of temperature-dependent constraints that become rigid as the liquid is cooled from high temperature to low temperature. This approach allows for calculation of T_g and m as a function of composition, i.e., the two independent parameters for describing the complete temperature dependence of liquid and supercooled liquid viscosity.[32] Here, T_g is defined as the temperature at which the shear viscosity is equal to 10^{12} Pa s and this isokom temperature has been shown to be equivalent to the calorimetrically measured T_g value for oxide glasses.[33] The fragility m is defined as the slope of the log η versus T_g/T curve at T_g:[34]

$$m \equiv \left.\frac{\mathrm{d}\log_{10}\eta}{\mathrm{d}(T_g/T)}\right|_{T=T_g} \quad (1)$$

Using Adam−Gibbs theory[35] and the energy landscape analysis of Naumis,[26,27] Gupta and Mauro derived expressions for calculating T_g and m as a function of composition.[29,30] $T_g(x)$ can be calculated, relative to that of some reference composition x_R, as

$$\frac{T_g(x)}{T_g(x_R)} = \frac{f(T_g(x_R), x_R)}{f(T_g(x), x)} = \frac{d - n(T_g(x_R), x_R)}{d - n(T_g(x), x)} \quad (2)$$

where $d = 3$ for a three-dimensional glass network and $f(T,x)$ is the number of low-frequency floppy modes (atomic degrees of freedom) for composition x at temperature T. The fragility index m can be calculated from the temperature derivative of $f(T,x)$:

$$m(x) = m_0\left(1 + \left.\frac{\partial \ln f(T,x)}{\partial \ln T}\right|_{T=T_g(x)}\right) \quad (3)$$

where $m_0 \approx 17$ is the fragility of a strong liquid.[29] The derivations of eqs 2 and 3 can be found in refs 29 and 30.

To understand the network topology and structure of the soda−lime−borate glass system, in this paper, we extend the topological model for the first time to a ternary composition space, viz, alkali−alkaline-earth−borate systems, and demonstrate how it can be applied to the discovery of new glass compositions in a system that has received little attention previously.[36] Through comparison of the model parameters and predictions with measured experimental data, we elucidate the microscopic topological origins of glass transition temperature and fragility. Besides studying the ternary system, we also prepare a sodium-free analog ($CaO-B_2O_3$) to evaluate the impact of sodium and calcium on the glass network. We determine the boron speciation in the glasses using ^{11}B magic-angle spinning (MAS) NMR spectroscopy and we compare the calculated and measured values of T_g and m.

2. Experimental Section

2.1. Sample Preparation. Twelve glass samples (see Table 1) were synthesized using analytical reagent-grade H_3BO_3 (Sigma−Aldrich, ≥99.5%), Na_2CO_3 (Sigma−Aldrich, ≥99.5%), $CaCO_3$ (Fluka, ≥99%), and Fe_2O_3 (Aldrich, ≥99.9%) powders. Most of the studied glasses contain 1 mol % Fe_2O_3, since they are also used in a parallel study that seeks to establish the influence of boron speciation on ionic transport. The transport properties will be studied using an inward cationic diffusion approach, which requires the presence of a polyvalent element in the glass.[37,38] Therefore, for the sake of comparison, we have also prepared iron-free samples.

Batches calculated to yield 400 g of glass were prepared for the iron-containing samples, whereas, for the iron-free samples, batches to yield 200 g of glass were prepared. The thoroughly mixed batches were melted in a covered $Pt_{90}Rh_{10}$ crucible at 1050−1150 °C for ∼15 min in an inductively heated furnace. Melting using a covered crucible and the relatively low melting temperatures and short times were chosen to minimize boron evaporation. Measurements of the weight loss due to melting indicate that the glasses are within 1−2 wt % of the desired compositions.

To obtain glasses, the melts were cast onto a brass plate and cooled in air to room temperature. The melts with the highest sodium contents (Ca10−Na35 and Ca10−Na35−Fe1) had to be pressed by another brass plate to avoid crystallization during cooling. We also attempted to prepare a glass with 40 mol % Na_2O, but this was not possible due to crystallization.[36] After determining the T_g value (see Section 2.3), the as-prepared glasses were annealed at their respective T_g values for 2 h to

(22) Senapati, U.; Varshneya, A. K. *J. Non-Cryst. Solids* **1995**, *185*, 289–296.
(23) Thorpe, M. F. *J. Non-Cryst. Solids* **1995**, *182*, 135–142.
(24) Georgiev, D. G.; Boolchand, P.; Micoulaut, M. *Phys. Rev. B* **2000**, *62*, R9228–R9231.
(25) Micoulaut, M.; Phillips, J. C. *Phys. Rev. B* **2003**, *67*, 104204.
(26) Naumis, G. G. *Phys. Rev. E* **2005**, *71*, 026114.
(27) Naumis, G. G. *J. Non-Cryst. Solids* **2006**, *352*, 4865–4870.
(28) Mauro, J. C.; Varshneya, A. K. *J. Am. Ceram. Soc.* **2007**, *90*, 192–198.
(29) Gupta, P. K.; Mauro, J. C. *J. Chem. Phys.* **2009**, *130*, 094503.
(30) Mauro, J. C.; Gupta, P. K.; Loucks, R. J. *J. Chem. Phys.* **2009**, *130*, 234503.
(31) Gjersing, E. L.; Sen, S.; Youngman, R. E. *Phys. Rev. B* **2010**, *82*, 014203.
(32) Mauro, J. C.; Yue, Y. Z.; Ellison, A. J.; Gupta, P. K.; Allan, D. C. *Proc. Natl. Acad. Sci. U.S.A.* **2009**, *106*, 19780–19784.
(33) Yue, Y. Z. *J. Non-Cryst. Solids* **2009**, *355*, 737–744.
(34) Angell, C. A. *Science* **1995**, *267*, 1924–1935.
(35) Adam, G.; Gibbs, J. H. *J. Chem. Phys.* **1965**, *43*, 139–146.
(36) Donohoe, L. M.; Shelby, J. E. *Phys. Chem. Glasses: Eur. J. Glass Sci. Technol. B* **2006**, *47*, 16–21.
(37) Smedskjaer, M. M.; Deubener, J.; Yue, Y. Z. *Chem. Mater.* **2009**, *21*, 1242–1247.
(38) Smedskjaer, M. M.; Mauro, J. C.; Yue, Y. Z. *J. Chem. Phys.* **2009**, *131*, 244514.

Table 1. Nominal Compositions and Properties of Investigated Glass Samples

	Nominal Composition (mol %)[a]						
notation	B_2O_3	CaO	Na_2O	Fe_2O_3	N_4 (±1%)[b]	T_g (K)[c]	m[d]
Ca10−Na5	84.85	10.1	5.05			708	
Ca10−Na15	74.75	10.1	15.15		37	775	
Ca10−Na25	64.65	10.1	25.25		46	764	
Ca10−Na35	54.55	10.1	35.35		41.3	716	
Ca10−Na5−Fe1	84	10	5	1	16	693	45 ± 2
Ca10−Na10−Fe1	79	10	10	1	24	756	49 ± 2
Ca10−Na15−Fe1	74	10	15	1	36	771	54 ± 3
Ca10−Na20−Fe1	69	10	20	1	40	768	58 ± 4
Ca10−Na25−Fe1	64	10	25	1	46	756	65 ± 5
Ca10−Na30−Fe1	59	10	30	1	43	740	56 ± 6
Ca10−Na35−Fe1	54	10	35	1	42	711	53 ± 3
Ca36−Fe1	63	36		1	43	912	

[a] The weight loss due to melting in the induction furnace was 1−2 wt %. [b] The ratio of tetrahedral to total boron (N_4) has been determined by ^{11}B MAS NMR. [c] The glass transition temperature (T_g) has been determined using differential scanning calorimetry (DSC) at 10 K/min, and the error in T_g associated with this method is generally ±2−3 K. [d] The fragility index (m) has been calculated using eqs 4 and 5.

diminish internal stresses. The isothermal annealing at T_g was followed by slow cooling to room temperature. Because of the hygroscopic character of the borate glasses, all samples were kept in glass or plastic containers with desiccant.

2.2. ^{11}B MAS NMR Spectroscopy. ^{11}B MAS NMR spectra were acquired using a JEOL Model JNM-ECA930 spectrometer that was equipped with a JEOL magnet (21.8 T) operating at a Larmor frequency of 298.2 MHz for ^{11}B. All MAS NMR spectra were acquired using a solid 10° pulse (1.4 μs). Crushed samples were taken in ZrO_2 rotors and were spun at 16 kHz in a 4-mm JEOL MQ/MAS probe. A recycle delay of 1 s was used and a total of 560−2000 free induction decays were averaged and Fourier-transformed to obtain each ^{11}B MAS NMR spectrum. The chemical shift for ^{11}B was externally referenced to $BF_3 \cdot Et_2O$.

2.3. DSC Measurements. The values of T_g and m were determined using a calorimetric method. The calorimetric measurements were performed with a differential scanning calorimetry (DSC) instrument (STA 449C Jupiter, Netzsch, Selb, Germany). The measurements were conducted in a purged argon atmosphere (40 mL/min). The isobaric heat capacity (C_p) curve for each measurement was calculated relative to the C_p curve of a sapphire reference material of comparable mass.

The samples were subjected to two runs of DSC upscans and downscans. The rates of the upscans and downscans were always equal, and the scan rate q was varied between 2 K/min and 30 K/min. The recorded heat flow of the first upscan reflects the enthalpy response of a sample with an unknown thermal history (i.e., an unknown cooling rate experienced by the sample during melt-quenching), whereas that of the second upscan reflects the enthalpy response of the sample with a well-defined thermal history (i.e., a known cooling rate). At the second upscan, the calorimetric fictive temperature (T_f) is defined as the cross point between the extrapolated straight line of the glass C_p curve before the transition zone and the tangent at the inflection point of the sharp rise curve of C_p in the transition zone. The value of T_f increases with increasing upscan rate, and the T_f value measured during an upscan rate of 10 K/min after a previous downscan at the same rate corresponds to the standard T_g value.[39] According to previous studies,[40] the dependence of the reciprocal DSC upscan rate on T_f corresponds to the temperature dependence of the equilibrium viscosity. Thus, we may write

$$\ln\left(\frac{q}{T_f^2}\right) = -\frac{E_g}{RT_f} + \text{constant} \quad (4)$$

where E_g is the activation energy for equilibrium viscous flow in the glass transition region and R is the ideal gas constant. The fragility m may then be calculated from E_g and T_g as[33]

$$m = \frac{E_g}{RT_g \ln 10} \quad (5)$$

3. Theoretical Approach

3.1. Network Structure and Topology. Pure B_2O_3 glass consists of corner-sharing BO_3 triangles, which combine to form three-membered boroxyl ring units. When alkali oxides are added to B_2O_3, there are two possible scenarios: (a) creation of a nonbridging oxygen (NBO), rupturing the linkage between two trigonally coordinated BO_3 groups; or (b) conversion of boron from a three-coordinated (B^3) to a four-coordinated (B^4) state without the creation of NBO. The ratio of B^4 to B^3 depends on the concentration of network modifiers, which causes many physical and chemical properties to vary nonmonotonically with composition. For example, T_g initially increases and later decreases with increasing alkali content.[41,42] This effect has been termed the "boron anomaly" by glass scientists, and numerous studies have been carried out by using NMR,[10−13] X-ray diffraction (XRD),[14,15] infrared (IR) spectroscopy[16] and Raman spectroscopy.[16,17] Besides the compositional effect, the change in boron speciation can also be induced by changes in pressure and temperature.[43−45]

Let us now consider the soda−lime−borate system. As a first approximation, we neglect the presence of iron in

(39) Yue, Y. Z. *J. Non-Cryst. Solids* **2008**, *354*, 1112–1118.
(40) Moynihan, C. T.; Lee, S. K.; Tatsumisago, M.; Minami, T. *Thermochim. Acta* **1996**, *280*, 153–162.
(41) Karsch, K. K. *Glastech. Ber.* **1962**, *35*, 234–243.
(42) Lower, N. P.; McRae, J. L.; Feller, H. A.; Betzen, A. R.; Kapoor, S.; Affatigato, M.; Feller, S. A. *J. Non-Cryst. Solids* **2001**, *293−295*, 669–675.
(43) Stebbins, J. F.; Ellsworth, S. E. *J. Am. Ceram. Soc.* **1996**, *79*, 2247–2256.
(44) Lee, S. K.; Mibe, K.; Fei, Y.; Cody, G. D.; Mysen, B. O. *Phys. Rev. Lett.* **2005**, *94*, 165507.
(45) Lee, S. K.; Eng, P. J.; Mao, H.-K.; Meng, Y.; Newville, M.; Hu, M. Y.; Shu, J. *Nat. Mater.* **2005**, *4*, 851–854.

the glasses and write the chemical formula as $x\mathrm{Na_2O}\cdot y\mathrm{CaO}\cdot(1-x-y)\mathrm{B_2O_3}$. Following Greenblatt and Bray[46] and Lower et al.,[42] we consider that the effect of CaO on boron speciation is the same as adding $\mathrm{Na_2O}$. In other words, the addition of CaO converts two trigonal B atoms to a tetrahedral state. In the regime of $x + y \leq 1/2$, we suggest that there are four network-forming species to consider in this system: (i) four-coordinated boron bonded to four bridging oxygens (B^4); (ii) three-coordinated boron bonded to three or two bridging oxygens (B^3); (iii) oxygen (O), including both bridging and nonbridging varieties; and (iv) network modifiers (Na and Ca) that create NBOs (M^{NB}). The modifiers that convert boron from B^3 to B^4 have only a charge-compensating role and are not considered as part of the network, i.e., by themselves they contribute neither degrees of freedom nor constraints. The effect of the charge-compensating ions is taken into account through the boron coordination change. The fact that we consider the modifiers that create NBOs as part of the network requires justification. In silicate glasses, the modified random network model of Greaves[47] suggests that the modifiers form clusters between the bridged SiO_4 units, to which they are linked primarily via the NBOs. The clustering of modifiers has been confirmed by molecular dynamics simulations.[48,49] Recently, such nonrandom distribution of bridging oxygens (BOs) and NBOs around modifiers has also been observed for boroaluminosilicate glasses.[50] The clustering of modifiers indicates that there could be a constraint on them, since they are not free to be randomly distributed in the network. In Section 4.2, it will be shown that the experimental T_g data can only be predicted by the topological model if point (iv) is built into the model.

Various structural models of borate glasses have been proposed in the literature. The models of Abe[51] and Beekenkamp[52] are based on the structure involving only B^3-O-B^3 and B^3-O-B^4 bridges, whereas B^4-O-B^4 bridges are unlikely to occur. In our topological model, we describe the boron speciation in terms of the random pair model of Gupta,[53] since it has proved successful across a wide range of modifier contents.[53,54] This model is based on three rules for network formation:

- BO_4 tetrahedra occur in corner-sharing pairs, i.e., there is one B^4-O-B^4 bridge for every pair. The B^4-O-B^4 angle within a pair is random.
- Pairs of BO_4 tetrahedra cannot be bound to each other.
- NBOs occur only in BO_3 groups and not in BO_4 groups.

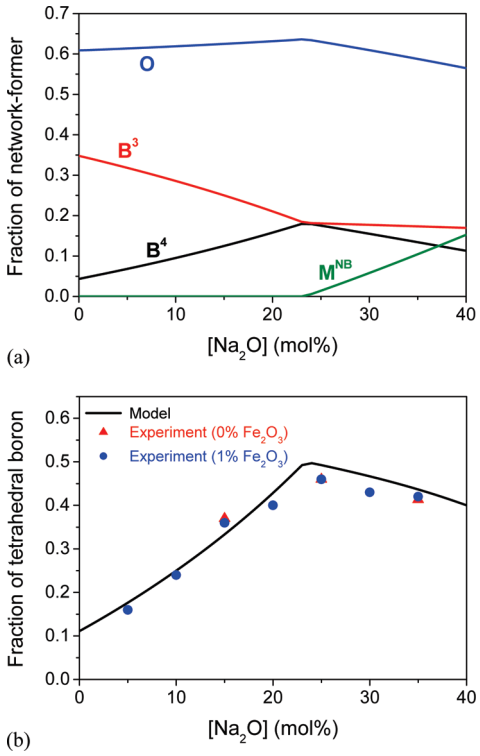

Figure 1. (a) Fraction of network-forming species and (b) boron speciation in the soda−lime−borate systems from Table 1, following the random pair model of Gupta.[53]

With these rules, the addition of alkali or alkaline-earth oxide will always result in the conversion of B^3 to B^4 when the modifier-to-boron ratio is $< 1/2$ ($(x+y)/[1-(x+y)] \leq 1/2$, i.e., $x + y \leq 1/3$). NBOs first begin to form when $x + y > 1/3$. Following Mauro et al.,[30] we calculate the fraction N of each network-forming species (see formulas in the Supporting Information). These fractions are plotted as a function of x in Figure 1a, in which we have set $y = 0.1$ (cf. Table 1).

3.2. Calculation of Glass Transition Temperature and Fragility. Next, we apply the temperature-dependent constraint model to calculate $T_g(x,y)$ and $m(x,y)$. To do so, we first identify and count the number of constraints associated with each distinct network-forming species. The different constraints are then ranked in terms of their relative bond strengths (i.e., constraint onset temperature). Equations 2 and 3 may then be applied to calculate $T_g(x,y)$ and $m(x,y)$, respectively. In the Results section, we compare these values with those obtained from experiments.

We consider the following types of bond constraints:

- α: B−O and $M^{NB}-O$ linear constraints. There are two α constraints at each oxygen.
- β: O−B−O angular constraints. There are five β constraints per B^4 to form a rigid BO_4 tetrahedron and three β constraints per B^3 to keep the BO_3 unit planar.
- γ: B−O−B angular constraints. There is one γ constraint at each oxygen.
- μ: additional modifier rigidity due to clustering effects. Based on the ensuing discussion, we consider two μ constraints per NBO-forming Na atom, whereas there are zero constraints for Ca.

(46) Greenblatt, S.; Bray, P. J. *Phys. Chem. Glasses* **1967**, *8*, 190–193.
(47) Greaves, G. N. *J. Non-Cryst. Solids* **1985**, *71*, 203–217.
(48) Huang, C.; Cormack, A. N. *J. Chem. Phys.* **1990**, *93*, 8180–8186.
(49) Huang, C.; Cormack, A. N. *J. Chem. Phys.* **1991**, *95*, 3634–3642.
(50) Wu, J. S.; Stebbins, J. F. *J. Non-Cryst. Solids* **2009**, *355*, 556–562.
(51) Abe, T. *J. Am. Ceram. Soc.* **1952**, *35*, 284–299.
(52) Beekenkamp, P. In *Physics of Non-Crystalline Solids*; Prins, J. A., Ed.; North−Holland, 1965.
(53) Gupta, P. K. In *Proceedings of the International Congress on Glass*; unpublished; New Delhi, India, 1986.
(54) Wright, A. C. *Phys. Chem. Glasses: Eur. J. Glass Sci. Technol. B* **2010**, *51*, 1–39.

The constraint onset temperatures are ordered such that

$$T_\gamma < T_g(0,0) < T_\beta(0,0) < T_\mu < T_\alpha \quad (6)$$

Here, the linear constraints freeze in at the highest temperature, because these bonds are the strongest. The μ constraint is considered to be the second strongest, since it is also two-body in nature. We assume that the β constraint onset temperature is dependent on the ratio of [Na_2O] to [CaO] (see reasoning in the Supporting Information):

$$T_\beta(x,y) = \left(\frac{2x}{2x+y}\right)T_\beta^{Na} + \left(\frac{y}{2x+y}\right)T_\beta^{Ca} \quad (7)$$

where T_β^{Na} is obtained from Mauro et al.[30] (T_β^{Na} = 740 K) and T_β^{Ca} is obtained from Donohoe and Shelby[36] (T_β^{Ca} = 910 K). These temperatures correspond to the T_g values for [Na_2O]/[CaO] ratios of infinity and zero, respectively. Following the structural analysis of Mozzi and Warren,[14] the O−B−O angle has a stronger constraint than the B−O−B angle, i.e., $T_\beta(0,0) > T_\gamma$. In fact, the B−O−B angular constraints freeze in at the lowest temperature, since T_γ can be estimated based on the Vogel temperature of B_2O_3, $T_\gamma \approx T_0(0,0)$ = 328 K.[30,55] The glass transition temperature of pure B_2O_3, $T_g(0,0)$, is 543 K.[56]

Following the constraint counting arguments above, the number of constraints per atom is given by

$$n(x,y) = 5N(B^4) + 3N(B^3) + 2N(O) + \frac{4x}{2x+y}N(M^{NB}) \quad (8)$$

in the glass transition range $T_\gamma < T_g(x,y) < T_\beta(x,y)$. The corresponding number of atomic degrees of freedom is

$$f(x,y) = 3 - n(x,y) = 3 - 5N(B^4) - 3N(B^3) - 2N(O) - \frac{4x}{2x+y}N(M^{NB}) \quad (9)$$

By combining eqs 2 and 9, the scaling of the glass transition temperature T_g with composition is given by

$$T_g(x,y) = \min\left[T_\beta(x,y), \frac{f(0,0)}{f(x,y)}T_g(0,0)\right] \quad (10)$$

The minimum function ("min") in eq 10 results from the breakdown of eq 9 when $T_g(x,y) > T_\beta(x,y)$, since eq 9 assumes that the β constraints are rigid. When the calculated T_g rises above the onset temperature of the β constraints, then this assumption is violated.

The temperature dependence of the constraints is modeled by the constraint onset function, $q_i(T)$, which is a measure of the rigidity of any constraint i as a function of temperature. Following Mauro et al.,[30] a discrete (unit step) form of $q_i(T)$ was used to calculate $T_g(x,y)$. However, since the calculation of fragility m involves taking the temperature derivative of $f(T,x,y)$ in eq 3, we must use a continuous form of $q_i(T)$ to calculate $m(x,y)$. According to the energy landscape approach, $q_i(T)$ can be computed as a continuous function of temperature,[57]

$$q_i(T) = \left[1 - \exp\left(-\frac{\Delta F_i^*}{kT}\right)\right]^{\nu t_{obs}} \quad (11)$$

where ΔF_i^* is the activation energy for breaking the i constraint, ν the vibrational attempt frequency, and t_{obs} the observation time. ΔF_i^* can be calculated from the constraint onset temperature T_i,[30]

$$\Delta F_i^* = -kT_i \ln[1 - 2^{-1/(\nu t_{obs})}] \quad (12)$$

Hence, νt_{obs} is the only unknown parameter. This parameter can be adjusted to study the cooling-rate dependence of the glass transition; however, we consider a constant value of νt_{obs} in this study, since we are interested in the composition dependence of fragility. Here, we will obtain the value of νt_{obs} by fitting to the experimentally measured values of fragility.

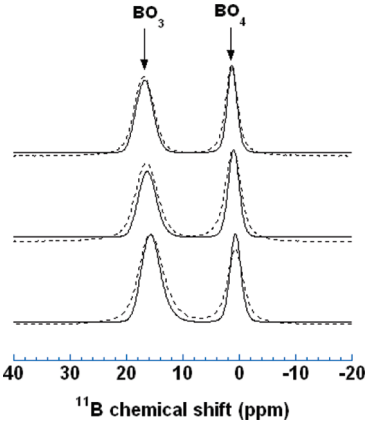

Figure 2. Representative high-field ^{11}B MAS NMR spectra of soda−lime−borate glasses with (dashed lines) and without (solid lines) 1 mol % Fe_2O_3. The spectra from top to bottom correspond to glasses with 35, 25, and 15 mol % Na_2O.

4. Results

4.1. Boron Speciation. The predicted boron speciation is now compared with experimental data obtained by ^{11}B MAS NMR spectroscopy. A representative set of high-field ^{11}B MAS NMR spectra of Na_2O−CaO−B_2O_3 glasses with 0 and 1 mol % Fe_2O_3 are shown in Figure 2. These spectra are characterized by a broad, almost-symmetric peak centered at ~16 ppm, corresponding to the B^3 sites and a relatively narrow symmetric peak centered at ~1 ppm, corresponding to the B^4 sites. The presence of 1 mol % Fe_2O_3 results in broadening of the two ^{11}B peaks, because of dipolar coupling between ^{11}B nuclear spin and unpaired spin of d-electrons in Fe (see Figure 2). However, quantitative analyses using spectral integration that includes all spinning sidebands over a wide frequency range indicate that no ^{11}B signal is lost due to such spectral broadening. The relative fractions of B^3 and B^4

(55) Avramov, I. *J. Non-Cryst. Solids* **2005**, *351*, 3163–3173.
(56) Moynihan, C. T. *J. Am. Ceram. Soc.* **1993**, *76*, 1081–1087.
(57) Gupta, P. K.; Mauro, J. C. *J. Chem. Phys.* **2007**, *126*, 224504.

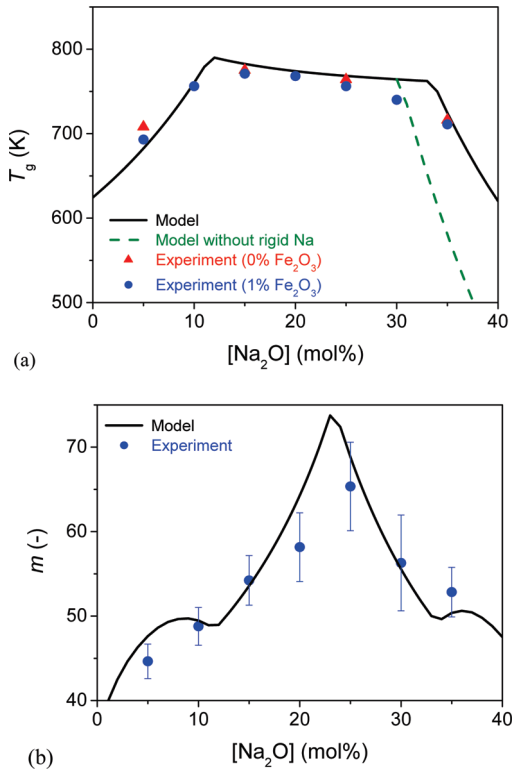

Figure 3. (a) Dependence of the glass transition temperature (T_g) on composition for $Na_2O-CaO-B_2O_3$ systems with 0 or 1 mol % Fe_2O_3. The lines show the computed $T_g(x,y)$ values using eq 10, assuming two rigid μ constraints per NBO-forming Na (solid line) or zero modifier constraints (dashed line). (b) Dependence of fragility (m) on composition for $Na_2O-CaO-B_2O_3$ systems with 1 mol % Fe_2O_3. The solid line shows the predicted $m(x,y)$, using the topological model with $\nu t_{obs} = 60$.

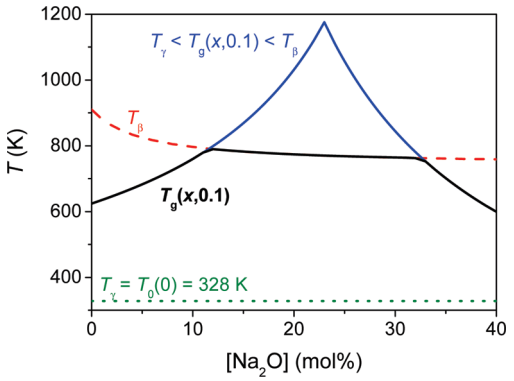

Figure 4. Dependence of the constraint onset temperatures and $T_g(x,y)$ on composition for the $x$$Na_2O$·0.1CaO·(0.9 − x)B_2O_3 system.

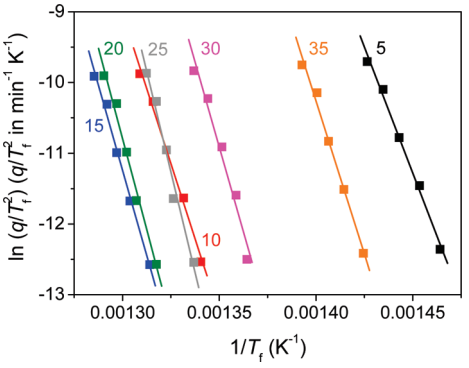

Figure 5. Plot of $\ln(q/T_f^2)$ as a function of $1/T_f$ for the $x$$Na_2O$·0.1CaO·-(0.89 − x)B_2O_3·0.01Fe_2O_3 systems with different concentrations of Na_2O (5, 10, 15, 20, 25, 30, or 35 mol %). The five data points for each composition correspond to heating/cooling rates of 2, 5, 10, 20, and 30 K/min, respectively. The solid lines represent linear fits to the data, and the fragility m can be calculated from the slope of each line, using eqs 4 and 5.

sites can be immediately obtained from the areas under the corresponding peaks in the ^{11}B MAS NMR spectra and are reported in Table 1 and Figure 1b. Figure 1b reveals good agreement between the experimental results and the predicted boron speciation following the random pair model of Gupta.[53] The BO_4 concentration peaks near the composition with $x + y = 1/3$, suggesting that the effect of CaO on boron speciation is indeed the same as that of Na_2O. The results also reveal that the addition of 1 mol % Fe_2O_3 has a negligible impact on boron speciation.

4.2. Glass Transition Temperature. The computed values of $T_g(x,y)$ using eq 10 are compared with experimental values of $T_g(x,y)$ for the systems investigated in this study (see Figure 3a). Note that the maximum in $T_g(x,y)$ does not correspond to the maximum in the fraction of tetrahedral boron (see Figure 1b). In Figure 3a, the modeled results are given under two different assumptions: no modifier rigidity (dashed curve) and two rigid μ constraints per NBO-forming Na atom and zero for Ca (solid curve). There are other possible assignments of modifier rigidity (Na and Ca can each have zero, one, two, or three constraints per atom), but the assumption of two rigid μ constraints per NBO-forming Na provides the best prediction of the experimental values. Furthermore, the assumption that sodium sets up a locally rigid environment due to clustering effects whereas calcium does not is in good agreement with previous findings for boroaluminosilicate glasses.[50] In Figure S1 in the Supporting Information, we also demonstrate good agreement between our modeling predictions and the experimental $T_g(x,y)$ values of Donohoe and Shelby.[36] Finally, Figure 3a shows that the addition of 1 mol % Fe_2O_3 reduces the glass transition temperature. When Fe_2O_3 was added to the glasses, the contents of all the other oxides were scaled proportionally. Therefore, addition of Fe_2O_3 results in a higher ratio of total modifier to B_2O_3 content in these glasses, which could explain the slight decrease in T_g.

To understand why our model is able to capture the composition dependence of the glass transition temperature for the soda−lime−borate systems, it is worthwhile to consider the composition dependence of the constraint onset temperatures. Following the discussion of Mauro et al.,[30] we set $T_\gamma = T_0(0,0) = 328$ K, where $T_0(0,0)$ is the Vogel temperature of pure B_2O_3.[55] Using eq 7, we have calculated and plotted $T_\beta(x,y)$, the onset temperature for the O−B−O angular constraints, as a function of composition in Figure 4. According to eq 2, thawing of the β constraints necessarily results in a decrease of $T_g(x,y)$. This pushes the glass transition temperature again below T_β, where the β constraints again become rigid. The net result of these competing effects is that the glass transition temperature is frozen at $T_\beta(x,y)$ until enough NBOs are formed to satisfy eq 2 at a new $T_g(x,y)$ below $T_\beta(x,y)$.

4.3. Liquid Fragility. Fragility, which is denoted as $m(x,y)$, is determined using DSC to establish the dependence of the fictive temperature (T_f) on the heating rate q (see Figure 5). Using eqs 4 and 5, we calculate m from the slope of each line and the resulting values are reported in Table 1 and Figure 3b. The fragility values are fit to our topological model, and we obtain $vt_{obs} = 60$. Figure 3b clearly shows that the experimental $m(x,y)$ values are in very good agreement with the calculated $m(x,y)$ values. The main feature is that fragility peaks at $x + y = 1/3$ (i.e., at the onset of NBO formation).

5. Discussion

We have shown that the addition of soda to a soda−lime−borate glass results in the conversion of BO_3 to BO_4 units until the total modifier content is ~33%; after that point, conversion of BO_4 to BO_3 and NBO occurs. These coordination changes may be quantitatively predicted by the random pair model of Gupta[53] and are identical to those found for binary alkali borates. Furthermore, we have found that substitution of the monovalent Na^+ ions by the divalent Ca^{2+} ions has a minimal effect on the boron speciation (compare boron speciation in the Ca10−Na25−Fe1 and Ca36−Fe 1 glasses in Table 1). The work of Donohoe and Shelby[36] supports our findings, since they have reported that the position of the maximum in T_g varies only slightly with the ratio of soda to lime. This indicates that only small variations in boron speciation occur as a function of the ratio of soda to lime. This is remarkable since a Na^+ ion is associated with a single BO_4 group, whereas a Ca^{2+} ion needs to be associated with two BO_4 groups (i.e., one Ca^{2+} ion per pair of BO_4 units in the Gupta random pair model). In contrast, Kamitsos et al.[58] have shown that the substitution of MgO for Na_2O in $MgO-Na_2O-B_2O_3$ glasses induces the formation of boroxyl rings, because of the destruction of diborate groups. Apparently, Mg^{2+} can relieve the rigidity of the diborate structure by polarizing the oxygen that bridges the two BO_4 groups, which causes the breakage of the B^4-O-B^4 bridge.[58] The fact that the Ca^{2+} ion does not have this effect may be due to its lower field strength. It is well-known that magnesium often behaves differently from the larger alkaline earths in glasses, because of its higher field strength.[38,59,60]

In the current model, we did not include a preference for sodium or calcium to induce the boron coordination change. To test the validity of this assumption, we build in such preferences in the model and then calculate $T_g(x,y)$ using eq 10. The results are shown in Figure S3 in the Supporting Information and clearly demonstrate that there is no significant preference for either sodium or calcium to cause the boron coordination change. The substitution of soda by lime has an impact on the absolute value of T_g (compare T_g of Ca36−Fe1 and Ca10−Na25−Fe1 in Table 1), viz, T_g increases as soda is replaced by lime. Since only a few percent of modifier is used for NBO formation in these glasses, the difference in T_g is most likely not a result of differences in Ca−O and Na−O bond strengths. Instead, the effects are explained by the impact of Ca on $T_\beta(x,y)$ in eq 7, i.e., the presence of Ca increases the rigidity of the O−B−O angular bonds.

The fragility of our soda−lime−borate systems increases with increasing sodium oxide content until $x + y \approx 1/3$ (see Figure 3b). Similarly, the fragility of binary alkali borate glasses increases with increasing alkali content for $x \leq 1/3$.[61−63] Compositions corresponding to $x + y = 1/3$ (or $x = 1/3$ in the binary case) have a peak in the number of tetrahedrally coordinated B atoms. This also corresponds to a peak in the number of O−B−O angular constraints (β constraints), since there are five β constraints for every tetrahedrally coordinated boron but only three β constraints per trigonally coordinated boron. From our modeling of $T_g(x,y)$, it is apparent that the glass transition in soda−lime−borate glasses is dominated primarily by the O−B−O angular constraints. As the number of these constraints peaks at $x + y = 1/3$, and since $T_\beta(x,y) \approx T_g(x,y)$ for most of the compositions under study, the fragility calculated from eq 3 must also display a maximum at $x + y = 1/3$. Hence, the nonmonotonic scaling of fragility with composition is yet another consequence of the so-called "boron anomaly" in these systems. Specifically, the microscopic origin of fragility of borate systems is the scaling of the concentration of O−B−O angles with composition.

The topological modeling approach presented in this paper represents an intermediate level of approach between traditional atomistic simulation techniques such as molecular dynamics and other more empirical macroscopic modeling. With constraint theory, we can isolate the key physics governing macroscopic properties such as glass transition temperature and fragility. Indeed, this work suggests that, with additional research, other thermal, mechanical, and rheological properties of glass may also be accurately predicted using constraint theory, since these properties are also strongly linked to the network topology. Constraint theory is already proving to be useful for efficiently exploring uncharted regions of composition space. For example, Figure 6a shows a complete ternary diagram for $T_g(x,y)$ and Figure 6b shows that for $m(x,y)$ in the $xNa_2O \cdot yCaO \cdot (1 - x - y)B_2O_3$ system. With constraint theory, these are simple analytical calculations. With traditional atomistic techniques (such as molecular dynamics), such calculations are currently infeasible. Note that the entire composition space in Figure 6 cannot be turned into glasses using standard laboratory melt-quenching techniques.[36] Hence, the glass-forming ability of the melts must also be considered when designing new glassy materials.

(58) Kamitsos, E. I.; Karakassides, M. A.; Chryssikos, G. D. *J. Phys. Chem.* **1987**, *91*, 1073–1079.
(59) Kroeker, S.; Stebbins, J. F. *Am. Mineral.* **2000**, *85*, 1459–1464.
(60) Shimoda, K.; Nemoto, T.; Saito, K. *J. Phys. Chem. B* **2008**, *112*, 6747–6752.
(61) Nemilov, S. V. *Glass Phys. Chem.* **1997**, *23*, 1–26.
(62) Chryssikos, G. D.; Duffy, J. A.; Hutchinson, J. M.; Ingram, M. D.; Kamitsos, E. I.; Pappin, A. J. *J. Non-Cryst. Solids* **1994**, *172−174*, 378–383.
(63) Matsuda, Y.; Fukawa, Y.; Kawashima, M.; Mamiya, S.; Kojima, S. *Solid State Ionics* **2008**, *179*, 2424–2427.

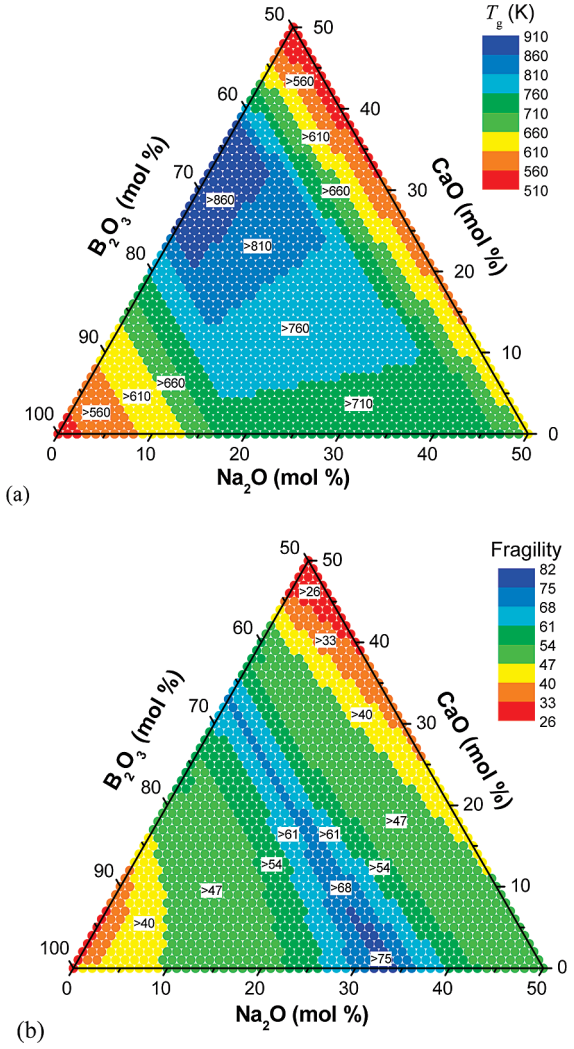

Figure 6. Model calculations of (a) $T_g(x,y)$ and (b) $m(x,y)$ for the $x\mathrm{Na_2O}\cdot y\mathrm{CaO}\cdot(1-x-y)\mathrm{B_2O_3}$ system. $T_g(x,y)$ is calculated using eq 10, whereas $m(x,y)$ is calculated using eqs 3 and 11 with $\nu t_{obs} = 60$. The topological modeling approach described in this paper is an efficient way to explore composition space without having to melt glasses across an entire phase diagram.

6. Conclusion

We have successfully combined topological modeling and experimental studies to gain insight into the network topology, structure, and properties of soda−lime−borate glasses. The addition of soda or lime to boric oxide results in a change in the boron coordination from three to four. This conversion occurs until the total modifier content is ∼33%, and further additions of modifier result in the formation of NBOs. These changes in boron speciation may be quantitatively predicted by the random pair model, i.e., our study has strengthened the universality of this model. In the NBO regime, comparison of computed and measured $T_g(x,y)$ values shows that the Na^+ ions set up a locally rigid environment of NBOs around themselves, whereas this does not seem to be the case for calcium, i.e., the two modifiers have significantly different effects on the glass structure. However, there is no preference for either sodium or calcium to cause the boron coordination change. The modeling approach also allows us to predict the scaling of fragility with composition, which shows a maximum at the peak concentration of four-coordinated boron. The microstructural origin of fragility is related to the number of O−B−O constraints in the system, which peaks at $x + y = 1/3$. Although the topological modeling approach presented here does not capture the minute level of detail captured by traditional atomistic simulation techniques,[64−66] it accurately captures the most relevant aspects of interactions that allow an accurate prediction of trends in the dynamic properties of glasses. The topological modeling approach is proving to be a valuable tool for exploring new composition spaces where glasses have not yet been melted.

Acknowledgment. The authors thank M. Jensen and R. Keding for technical assistance and M. Potuzak, A. J. Ellison, and Q. J. Zheng for valuable discussions. This work was supported by the International Doctoral School of Technology and Science at Aalborg University (under Ph. D. Stipend No. 562/06-FS-28045).

Supporting Information Available: Additional information on the modeling details and results as noted in the text. This material is available free of charge via the Internet at http://pubs.acs.org.

(64) Pedone, A.; Malavasi, G.; Cormack, A. N.; Segre, U.; Menziani, M. C. *Chem. Mater.* **2007**, *19*, 3144–3154.
(65) Pedone, A.; Malavasi, G.; Menziani, M. C.; Segre, U.; Cormack, A. N. *Chem. Mater.* **2008**, *20*, 4356–4366.
(66) Wondraczek, L.; Mauro, J. C. *J. Eur. Ceram. Soc.* **2009**, *29*, 1227–1234.